INTERNATIONAL JOURNAL OF AUTOMOTIVE AND MECHANICAL ENGINEERING
ISSN: 2229-8649 e-ISSN: 2180-1606
VOLUME 23, ISSUE 1, 2026, 13393 - 13404
DOI: https://doi.org/10.15282/ijame.23.1.2026.18.1016

RESEARCH ARTICLE

Investigation of impact factors in frontal collisions involving powered two-wheelers and cars

Yi Pang[1], Shaw Voon Wong[1*], Yong Han[2], Zulhaidi Jawi[3], Yahaya Ahmad[3], Kean Sheng Tan[4], Azizan As'arry[1], Qiuyun Mo[5], Tao Jiang[5]

[1]Department of Mechanical and Manufacturing Engineering, Universiti Putra Malaysia, 43400 Selangor, Malaysia
[2]School of Mechanical and Automotive Engineering, Xiamen University of Technology, 361024 Xiamen, China
[3]Malaysian Institute of Road Safety Research, 43000 Kajang, Malaysia
[4]National Defense University of Malaysia, 57000 Kuala Lumpur, Malaysia
[5]School of Mechanical and Electrical Engineering, Guilin University of Electronic Technology, 541004 Guilin, China

Abstract – Powered two-wheelers (PTWs) are highly vulnerable in road traffic accidents, with frontal collisions with cars frequently resulting in severe or fatal rider head injuries. However, while most research has focused on vehicle collisions and head injuries, studies on the influencing factors of rider head injuries in collisions where the vehicle front impacts the powered two-wheeler remain relatively limited. This study employs an orthogonal experimental design to conduct a simulation analysis of frontal collisions between cars and PTWs (motorcycles and electric two-wheelers). It investigates the impact of multiple factors, including vehicle speed, collision angle, and vehicle type, on rider head injuries. By reconstructing typical traffic accidents and combining multi-body dynamics models with human dummy models, the study quantifies variations in the Head Injury Criterion (HIC15) and the 3-millisecond acceleration peak (3 ms Clip). Results from the range analysis indicate that vehicle speed is the primary factor influencing HIC15 (Range value of 835.29), while collision angle most significantly affects the 3 ms Clip (Range value of 70.60). The research reveals significant differences in rider head injuries under various collision conditions and quantifies vehicle speed as the dominant factor for severe head injuries (HIC15). Consequently, it is recommended that accident mitigation strategies prioritize speed-control measures to reduce rider mortality effectively.

Article History
Received : 21 April 2025
Revised : 30 January 2026
Accepted : 13 February 2026
Published : 14 March 2026

Keywords
Frontal collision accident
PTW
Head injury analysis
Accident reconstruction

1. Introduction

According to the World Health Organization's "Global Status Report on Road Safety 2023", over half of United Nations member states worldwide have achieved reductions in road traffic accidents. However, the ASEAN region presents a distinct traffic safety pattern. Latest data from ASEAN-NCAP (2026-2030) reveals that fatalities among PTW riders, the predominant road user group in the region (constituting 80% of total users), have increased markedly [1-2]. Among collision-type categorized traffic incidents, lateral PTW collisions involving frontal automobile impacts account for the highest proportion. These collisions predominantly occur at intersections or during lane changes. The exposed structure and insufficient lateral protection of motorcycles exacerbate injury severity in such scenarios, underscoring the critical need for an in-depth investigation of the collision mechanisms of PTWs subjected to frontal impacts from automobiles. Head injuries are the primary cause of fatalities in traffic accidents, accounting for most fatal injury types [3-7]. Therefore, research on head injuries in frontal collisions is of significant practical importance for ASEAN regions and areas with high PTW usage, especially in developing effective safety protection measures and optimizing traffic safety regulations.

Due to the numerous interconnected factors between cars, PTWs, and riders, simulation results for such accidents can vary considerably depending on collision conditions. To accurately analyze dynamic injuries in rider collisions, previous research has employed various approaches. Wang et al. [8] enhanced human finite element models and multi-scenario simulation systems to reconstruct 20 accidents. Duan et al. [9] analyzed characteristics of craniocerebral injuries in road traffic accidents in Southwest China, combining patient medical records, CT scan data, and accident scene records. Baker et al. [10] provided a comprehensive review of rider head injuries and impact characteristics, highlighting multibody simulation and experimental verification as crucial tools for accident reconstruction. Fahlstedt et al. [11] compare and evaluate differences in head kinematics between the TNO and THUMS models in pedestrian accident situations. Wang et al. [12] developed a multi-objective optimization framework combining Uniform Latin Hypercube sampling and machine learning models to reduce electric bicycle riders' HIC15 and tibial injury values. Gao [13] studied rider head kinematic responses and injury risks in electric bicycle-car collisions using decision tree models, simulating 1,512 accident scenarios and revealing the significant impact of initial vehicle speed and collision angle on HIC15. Chen et al. [14] analyzed the impact of different riding postures on head injuries of child passengers on electric two-wheelers, finding that reverse seating significantly increases fatal head injury risks. Baker et al. [15] investigated the effect of parameter uncertainty on head kinematic responses and injury predictions, discovering significant differences in the dynamic distribution during head collisions with vehicles and with the ground.

With the ongoing development of finite element techniques, recent research has primarily explored the formation of craniocerebral injuries from perspectives including sports medicine, blunt force trauma, infant protection, automotive safety, and injury prevention [16-20]. However, research on the morphology and mechanisms of cranial brain injuries in

*CORRESPONDING AUTHOR | S. V. Wong | ✉ wongsv@upm.edu.my

PTW riders is limited. Currently, there are two primary standards for evaluating head injuries: one based on kinematics, including Head Injury Criterion (HIC), Brain Injury Criterion, and Head Impact Power, and another simulating brain tissue mechanical response, such as Von Mises stress, Maximum Principal Strain, and Cumulative Strain Damage Measure [21-23]. However, a systematic investigation into how multiple collision variables interact to influence rider head injury risks is still missing from the current literature. This study treats the above-mentioned factors as different initial collision conditions and conducts simulation tests of car-PTW collisions. The goal is to use a simulation analysis method that allows a unified examination of the effects on rider motion and injury across various conditions, and to explore how these effects change. This approach lays the foundation for the development of appropriate rider protection measures.

2. Materials and Methods

In car-PTW collision accident research, the head, as the body part with the highest fatality rate, has received extensive attention [24-30]. Due to the singular nature of current head injury assessment indicators (kinematic indicators and brain tissue mechanical response), they often fail to reflect head injury characteristics comprehensively. Therefore, this paper proposes a systematic analysis method based on orthogonal experimental design, by constructing a multi-factor evaluation system to comprehensively study the influence mechanism of factors such as vehicle speed, collision angle, and vehicle type on riders' head injuries, aiming to provide a theoretical basis for optimizing rider protection measures and accident liability determination. The specific research method is shown in Figure 1.

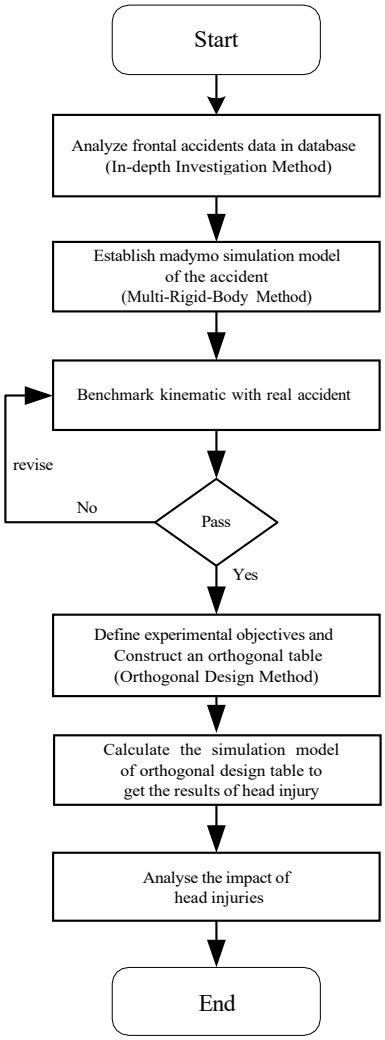

Figure 1. Method flowchart

2.1 Accident Information

Case 1: On July 12, 2021, on a two-way four-lane road, a parked car waiting to start hit an electrically powered two-wheeler (ETW) moving horizontally (Figure 2(a)). Due to the low speed, the accident did not cause any casualties.

Case 2: On May 3, 2021, at an intersection, a high-speed horizontally traveling car collided with a longitudinally traveling ETW (Figure 2(b)). The accident resulted in serious injury/death of the ETW rider.

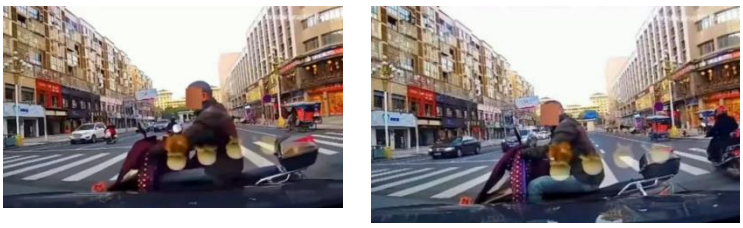

(a) Case 1

(b) Case 2

Figure 2. Video screenshots illustrating the different scenarios

(a) Accident case 1 reconstruction

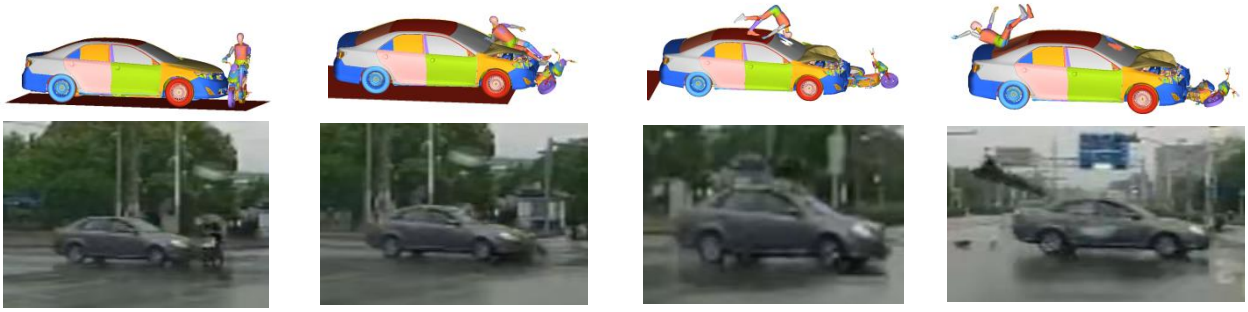

(b) Accident case 2 reconstruction

Figure 3. Accident reconstructions for (a) Case 1 and (b) Case 2

In case 1, since no one was injured in the accident and the speed was low, the corresponding Abbreviated Injury Scale (AIS) was level 1, the HIC was below 500, and the simulation speed was set to 10 km/h. Since the electric two-wheeler was essentially stationary when the accident occurred, while the car was moving at 10 km/h and the electric two-wheeler was at 0 km/h, the kinematic response of the rider throughout the collision and the car's deformation damage were consistent with the video information. Specifically, validation was performed by frame-by-frame comparison of the rider's kinematic trajectory. Key visual markers, including the rider's body posture, rotation angle, and the relative position of the head during the flight phase, were aligned with the CCTV footage at synchronized time steps to ensure high fidelity. The process comparison image is shown in Figure 3(a). In case 2, since the electric two-wheeler rider suffered serious injury or fatality in the accident, the corresponding AIS is level 6, so the collision speed in the simulation is set to 80 km/h. When the car is traveling at 80 km/h and the electric two-wheeler at 20 km/h, the kinematic response of the rider throughout the collision, as well as the car's deformation and damage, are consistent with the video. The process comparison image is shown in Figure 3(b). As shown in Figure 3, at 10 km/h, the dummy's head injury is very small, and

the AIS level corresponding to this HIC is 1. When the speed reaches 80 km/h, the injury to the dummy's head increases to 5756.23, and the AIS level corresponding to this HIC value is 6. The head acceleration is shown in Figure 4. Based on the reconstruction of the above two accident cases, the following conclusions can be drawn: When the relative collision speed of motor vehicles is around 10 km/h, the rider's head injury is minor, not exceeding AIS level 1. However, when the relative collision speed reaches or exceeds 80 km/h, the rider's head injury reaches AIS level 6. Therefore, 10 km/h and 80 km/h are used as boundary speeds for analysis, i.e., speeds below 80 km/h. For relative collision speeds, the maximum speed for cars is set at 50 km/h, while for PTWs, it is limited to 30 km/h.

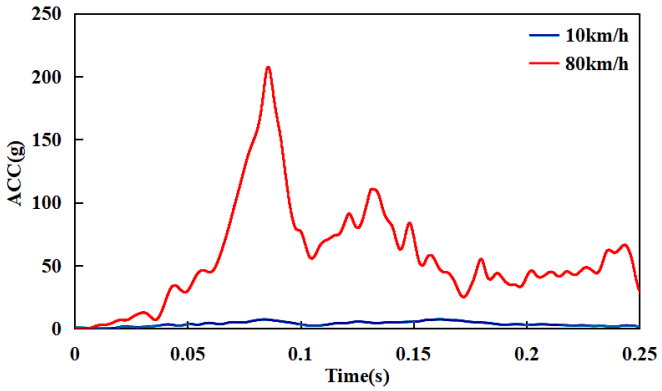

Figure 4. Head acceleration in the simulation model (ACC denotes resultant acceleration)

2.2 Multi-Rigid Body (PTW and Human Body) Model Setup

In the reconstructed accident cases, the damage to the ETW was relatively minor. After a detailed recording of ETW parameters in the parking lot, modeling was conducted based on the measured dimensions, enabling an accurate reconstruction of the accident sequence. Since the ETW mainly consists of the front wheel, head, frame, and rear wheel, these four parts can be modeled as a multi-rigid-body system, simplifying the model somewhat. Among the four main components of the ETW, the front fork and front wheel are responsible for steering. In Madymo software, the connection between the front fork and the front wheel is defined as a kinematic hinge with a revolute joint, enabling relative rotation with respect to the entire multibody system. In addition to the rotation of the front fork and front wheel relative to the ETW model, this ETW model, as a multi-rigid body system, can also undergo translational and rotational motion relative to the reference space. Through a free joint connection (JOINT.FREE), the center of mass of the ETW multi-rigid body model is set as the origin of the rigid body coordinate system and the reference point relative to the reference space. At this point, the ETW multi-rigid-body model has 6 degrees of freedom in the spatial coordinate system. The construction of this model is achieved by establishing multiple ellipsoids fixed on kinematic hinges, where the four major components - front wheel, front fork, frame, and rear wheel - are all characterized by ellipsoid structures. By defining rotational hinges at the front wheel, the front fork, and the rear wheel, the ETW model's movement and steering functions are realized. The detailed ETW assembly model is shown in Figure 5(a). The mass, moment of inertia, center of mass height, and initial collision speed of the ETW are assigned to the multi-rigid body model.

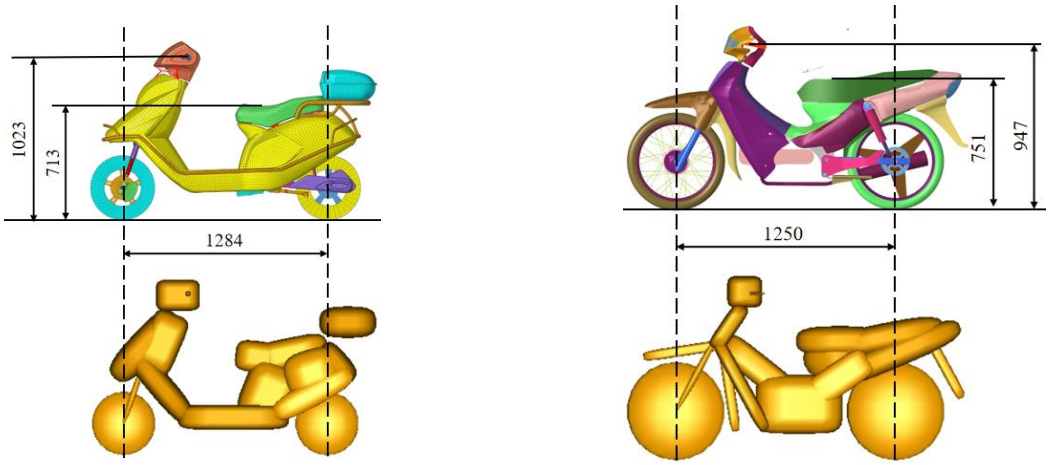

(a) ETW (b) Motorcycle

Figure 5. Multiple rigid-body models are used for the simulation

The motorcycle model used is based on one of Malaysia's national motorcycles, an early version of the Kriss110, which is the most common type of motorcycle used for daily transportation in ASEAN countries. As with the ETW modeling method, the established motorcycle simulation model shown in Figure 5(b) has been compared with the finite

element simulation model. Two generic vehicle models were employed to represent the opposing collision objects: a Sedan and an SUV. The key distinction lies in their mass and front-end geometry; the SUV is 1.6t, and the sedan is 1.3t. The sedan model features a lower hood leading edge height, whereas the SUV model has a higher front-end profile. These geometric parameters were set to investigate how the height of the primary impact point affects the rider's post-impact kinematics, while the vehicles themselves were treated as rigid bodies.

Madymo provides a series of human body models. This paper decided to use the 50th percentile male pedestrian model and adjust its height to match the rider's height in the real accident, i.e., 1.75 meters and 75 kilograms. The software automatically adjusts mass, geometry, and other parameters accordingly, then adjusts the human joints to simulate the appropriate sitting posture on the previously modeled E2W. This modified human model better represents the Chinese 50th percentile male than the original Madymo 50th percentile male, as it is slightly smaller than the original pedestrian model representing the average European male. The dummy and motorcycle are hinged together via a free joint, and the dummy's position is adjusted as shown in Figure 6.

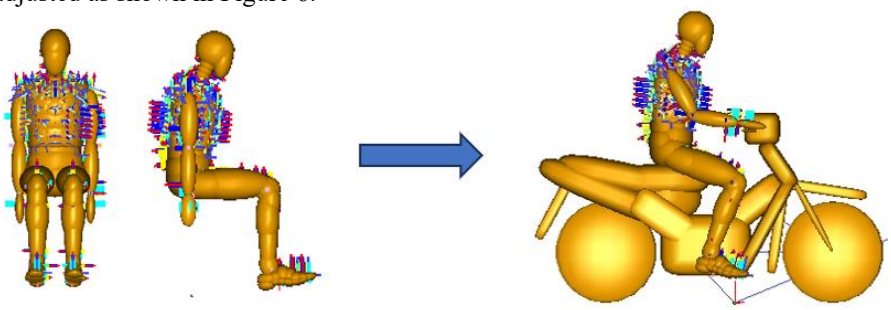

Figure 6. 50th percentile (seated) male dummy

2.3 Influencing Factors

The process of a car-two-wheeler collision is highly complex, involving numerous interrelated factors between the car, the two-wheeler, and the rider. The Madymo simulation model is shown in Figure 7. Due to the varied and intricate nature of such accidents, the simulation results can differ significantly depending on the collision conditions. To accurately analyze the collision dynamics and injuries in car-two-wheeler collisions, it is essential to consider multiple variables. These include the car model, the type of powered two-wheeler, the car's collision speed, the two-wheeler's driving speed, the point of impact, and how these factors influence the rider's motion and injury patterns during the collision. This study analyzed two distinct types of PTWs: the internal combustion engine motorcycle (referred to as 'Motorcycle') and the electrically powered two-wheeler (referred to as 'ETW'). These two types differ significantly in mass distribution, structural stiffness, and power source, all of which are critical factors in collision dynamics. Given these complexities, this study treats the aforementioned factors as distinct initial collision conditions and conducts simulations of car-two-wheeler collisions. The goal is to develop a simulation analysis method that enables a unified examination of the effects on rider motion and injury across various conditions, while exploring how these effects change. The speed, angle, and position of the vehicle and Vulnerable Road User (VRU) are adjusted using free hinges to ensure that the point of collision aligns with the center of the dummy's head along the vehicle's longitudinal axis, as shown in Figure 8.

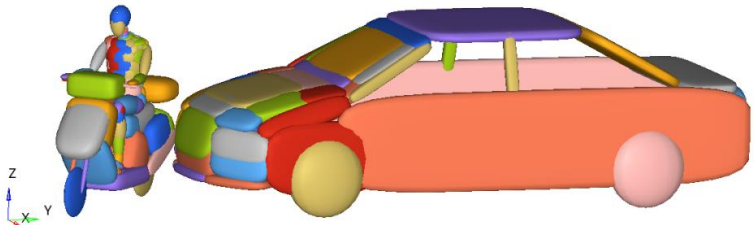

Figure 7. Car-PTW frontal collision

As shown in Figure 9, in China, according to the VRU-TRAVi (VAU Traffic Accident Database with Videos), when a car collides with a PTW, the car's speed is between 20 and 50 km per hour, and the PTW's speed is in the range of 10-30 km per hour. Since the collision angles between PTW and the car vary in accidents, there are significant differences in the impact positions on the rider and the vehicle, as well as post-collision movement patterns, all of which affect injury severity. Research shows that the collision angles between PTW and car mainly fall into two categories: the first category includes angles of 45°, 90°, and 135° between the directions of the car and PTW, while the second category includes angles of 30°, 60°, 90°, 120°, and 150°. Based on the concept of uniform design, this paper adopts the first category. The study first identifies the key factors influencing car-to-PTW collisions, including car model, collision speed, powered two-wheeler driving speed, powered two-wheeler type, and collision location, which serve as the initial variables for the simulation tests. To efficiently and comprehensively analyze these factors, the study employs an orthogonal experimental design in the simulation tests, making the research process both economical and efficient. The main car models involved in actual accidents are then simulated and modeled, followed by collision simulation tests. These tests analyze how

variations in different factors impact the simulation results. The influence of various factors on the dynamic response of motorcycle riders is studied through simulation experiments.

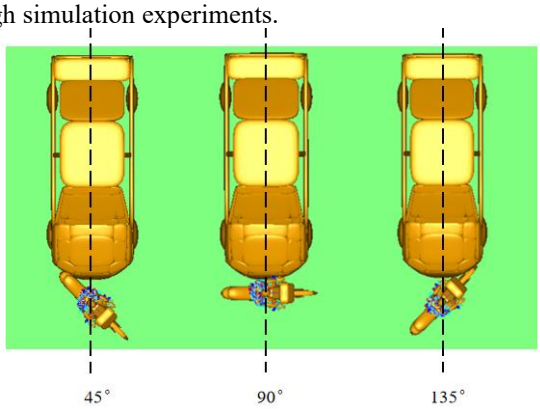

Figure 8. Collision angle diagram

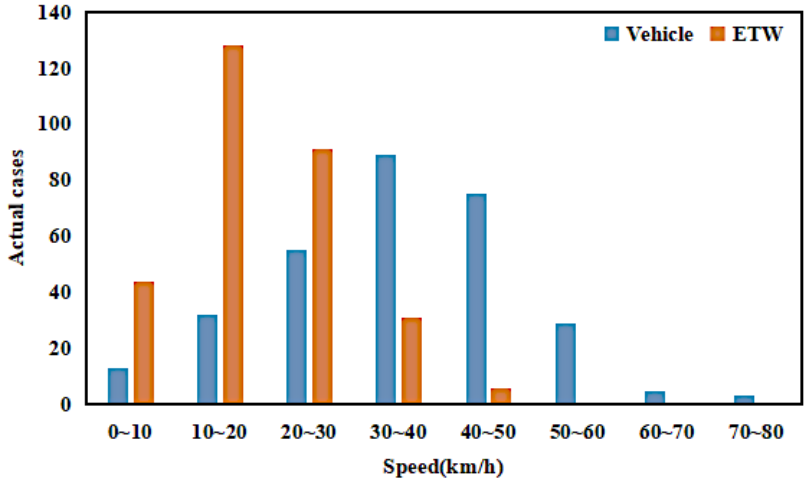

Figure 9. Collision speed

2.4 Orthogonal Experimental Design

The influencing factors in car-PTW collision accident simulation tests are divided into five key variables: the car model involved in the accident, the type of PTW, the car's collision speed, the PTW's traveling speed, and the PTW's collision angle. To study the influence of these five factors on the simulation results and analyze the rider's collision movement and injury severity, it is impractical to conduct a complete combinatorial test of all factors. To efficiently and comprehensively analyze these factors, car-PTW collisions are simulated using an orthogonal experimental design, systematically assessing the influence of multiple factors on collision outcomes while significantly reducing the number of tests. The frontal collision analysis matrix would require the calculation of 108 simulation models. However, through the L_{18} orthogonal array design, the number of calculation conditions can be greatly reduced to 18 models, and statistical analysis can be performed on the obtained dummy injury values to find the factors related to frontal collision that have the greatest impact on dummy injury in accidents. The analysis of these factors and their respective levels is shown in Table 1.

Table 1. Design Parameters and Collision Test Levels

Factors	Level 1	Level 1	Level 1
Vehicle Type	Sedan(c1)	SUV(c2)	
PTW Type	Motorcycle(b1)	Electric two wheel(b2)	
Vehicle Speed	20 km/h(s1)	35 km/h(s2)	50 km/h(s3)
PTW Speed	10 km/h(p1)	20 km/h(p2)	30 km/h(p3)
Collision Angle	90°(a1)	135°(a2)	45°(a3)

4. Results and Discussion

4.1 Simulation Animation

In previous collision simulation studies, certain factors influencing the calculation results were not uniformly analyzed, and some were even overlooked. This oversight has often led to inconsistent simulation outcomes with the actual accident

process. To address this, this chapter investigates the simulation analysis method for two-wheeler collisions using a human-vehicle-road coupling system model. It examines the multiple factors affecting accident simulation results and explains their systematic influence on these outcomes. According to the orthogonal experimental design method, the collision test between a car and a two-wheeled vehicle is simulated and studied below. The calculation conditions of the orthogonal experimental design and the collision simulation animation results of the car and PTW are shown in Figure 10.

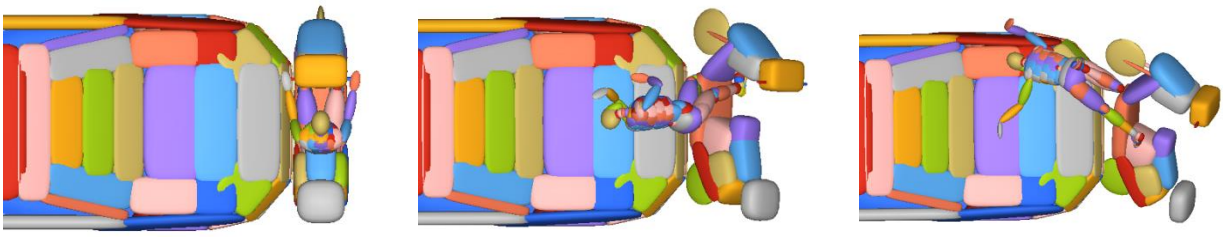

(a) 0 ms (b) 120 ms (Maximum acceleration moment) (c) 300 ms

Figure 10. Simulation results in orthogonal test 18

4.2 Range Analysis Method

The range analysis method for orthogonal experimental design can be used to evaluate simulation test results. The range is the difference between the maximum and minimum average test indicator values at each level in each column. Within the test range, the columns are arranged in descending order according to their influence on the test indicators. If the range value of a column is the largest, it indicates that the change in the numerical value of that column has the greatest impact on the change of the test indicator within the test range. Therefore, the influence of each column on the test indicator can be evaluated by the range value, and the columns are ranked from largest to smallest. Let the test value of factor m at level j be Y_i, and let K_j^m be the average test value of factor m at level j. The overall sum of the simulation results is denoted as K, the average as k_j^m, and the range as R^m. These are used to evaluate the impact of factors on the test, with the expressions given in Eqs. (1-3).

$$K = \sum_{i=1}^{n} Y \tag{1}$$

$$k_j^m = \frac{1}{n}\sum_{i=1}^{n} Y \tag{2}$$

$$R^m = max\left(k_j^m\right) - min\left(k_j^m\right) \tag{3}$$

In Eq. (1-3), the subscript i = 1, 2..., n represents the number of tests, the superscript m represents different influencing factors, and j represents different levels of factor m. The range method is simple to calculate, requiring only a comparison of the maximum and minimum values for each factor level. It can efficiently determine the influence of various factors on the test results.

4.3 Simulation Results of Each Scheme

The 3 ms Clip and HIC15 exhibit distinct patterns in assessing head injuries in car-PTW collisions, stemming from their different responses to the nature of impact forces. The 3 ms Clip is more sensitive to violent acceleration outbursts in a short time, while HIC15 reflects the cumulative effect of acceleration over a longer period. Based on the parameters set for each scheme, the 3 ms Clip and HIC15 values obtained through simulation are shown in Table 2, where the units of speed, angle, and 3 ms Clip are km/h, degrees (°), and the acceleration of gravity(g), respectively. The 3-ms clip measures peak acceleration over a very short time interval (3 milliseconds), which is highly sensitive to instantaneous forces. If a collision produces steep acceleration peaks within this short time, the 3-ms clip value will be high. On the other hand, HIC15 considers acceleration over a longer period (15 milliseconds). It calculates an integral value that reflects the overall acceleration curve, rather than just the peaks. If the acceleration is spread over a longer period, or if the peaks are less pronounced, the HIC15 value may be lower, even if the 3 ms Clip is high. Among them, the scheme with the maximum injury is the 9th group, and the scheme with the minimum injury is the 4th group. The large difference in values between them stems from the fact that scheme 4 involves only slight contact, while scheme 9 involves a death or serious injury. According to Table 2, the results of the range analysis are shown in Table 3.

Table 2. L_{18} Orthogonal Array layout and test results

Test No.	Type of car	Type of PTW	Car Speed	PTW Speed	Angle of Collision	3 ms Clip	HIC15
1	1 (Sedan)	1 (Motor)	1(20)	1(10)	1(90)	9.27	3.26
2	1 (Sedan)	1 (Motor)	2(35)	2(20)	2(135)	33.40	41.43
3	1 (Sedan)	1 (Motor)	3(50)	3(30)	3(45)	10.71	5.29
4	1 (Sedan)	2 (ETW)	1 (20)	2 (20)	3 (45)	3.75	0.31
5	1 (Sedan)	2 (ETW)	2 (35)	3 (30)	1 (90)	13.37	5.94
6	1 (Sedan)	2 (ETW)	3 (50)	1 (10)	2 (135)	83.70	1031.00
7	2 (SUV)	1 (Motor)	1 (20)	3 (30)	2 (135)	87.51	560.73
8	2 (SUV)	1 (Motor)	2 (35)	1 (10)	3 (45)	27.21	40.19
9	2 (SUV)	1 (Motor)	3 (50)	2 (20)	1 (90)	81.49	2064.66
10	2 (SUV)	2 (ETW)	1 (20)	1 (10)	1 (90)	11.52	6.21
11	2 (SUV)	2 (ETW)	2 (35)	2 (20)	2 (135)	99.94	1601.39
12	2 (SUV)	2 (ETW)	3 (50)	3 (30)	3 (45)	20.70	24.83
13	1 (Sedan)	1 (Motor)	1 (20)	1 (10)	3 (45)	4.46	0.60
14	1 (Sedan)	1 (Motor)	2 (35)	2 (20)	1 (90)	90.45	697.15
15	1 (Sedan)	1 (Motor)	3 (50)	3 (30)	2 (135)	123.09	972.26
16	2 (SUV)	2 (ETW)	1 (20)	2 (20)	2 (135)	67.50	377.55
17	2 (SUV)	2 (ETW)	2 (35)	3 (30)	3 (45)	4.70	0.36
18	2 (SUV)	2 (ETW)	3 (50)	1 (10)	1 (90)	96.76	1862.36

Table 3. Head Injury Range Results

Range Analysis	Range				
Parameters	R1	R2	R3	R4	R5
3 ms Clip (g)	13.90	7.29	24.56	23.05	70.60
HIC	605.67	58.26	835.29	472.59	761.33

4.4 Analysis of Minimum and Maximum Head Injuries

Based on the simulation results in Table 2, the minimum head injury scenario is Test 4, while the maximum head injury scenario is Test 9. For Test 4, the car speed is 20 km/h, the ETW (Powered Two-Wheeler) speed is 20 km/h, and the collision angle is 45°. When the PTW and car are moving in the same direction, if the PTW's speed equals or exceeds the car's speed, the car can contact the PTW rider's head. Compared to Test 16, in a 135° collision, both the PTW and car are moving toward each other, resulting in a relatively higher absolute collision speed due to the addition of their relative speeds. Test 9 represents the most severe head injury scenario, where the SUV speed is 50 km/h, the motorcycle speed is 20 km/h, and the collision angle is 90°. When an SUV collides head-on with a PTW, the motorcyclist suffers more severe injuries than in other scenarios due to inertial effects, as shown in Figure 11.

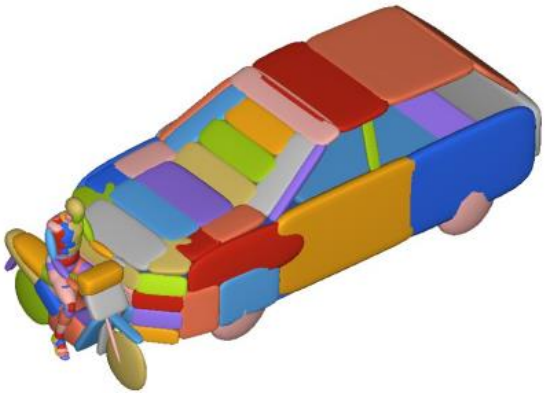

Figure 11. Simulation results of orthogonal test 9

4.5 Analysis of Influencing Factors

When a car collides with a PTW, especially from the side or at a certain angle, the rider may experience a sudden, violent impact. If the impact is violent and short in duration, the 3-ms clip will show a higher value, while the HIC15 indicates a lower overall risk of injury. The materials and structures involved in the collision (such as helmets or vehicle structures) also have different effects on both indicators. The divergence in influencing factors for HIC15 and 3 ms Clip can be attributed to their distinct physical definitions. HIC15 represents the cumulative damage over a time interval and is intrinsically linked to the system's total kinetic energy. Since kinetic energy is proportional to the square of the velocity, vehicle speed naturally becomes the dominant factor for HIC15. In contrast, the 3 ms Clip reflects the peak instantaneous acceleration, which is highly sensitive to the stiffness of the impact surface. The collision angle dictates the rider's kinematic trajectory and the specific point of impact on the vehicle. Varying angles determine whether the rider's head strikes the relatively compliant hood (resulting in a lower peak) or the rigid structural components, such as the A-pillar or the windshield frame (resulting in a sharp acceleration

spike). Therefore, the collision angle plays a more decisive role in determining the magnitude of the 3 ms Clip than speed alone. As shown in Figure 12, R1 reflects the type of car, R2 reflects the type of PTW, R3 reflects the speed of the car, R4 reflects the speed of the PTW, and R5 reflects the influence of the collision angle. Therefore, the order of primary and secondary influencing factors for rider head HIC15 injury is: R3 > R5 > R1 > R4 > R2, indicating that car speed is the most important factor affecting head HIC15 injury, while PTW type has the least influence. The order of primary and secondary influencing factors for the 3 ms clip injury is: R5>R3>R4>R1>R2, indicating that the collision angle has the greatest impact on the head 3 ms Clip injury, while the type of PTW has the least influence. To validate these observations, our findings align with those of Gao [13], who also identified vehicle speed and collision angle as significant predictors for head injury risks. This consistency confirms the reliability of the orthogonal simulation results presented in this study.

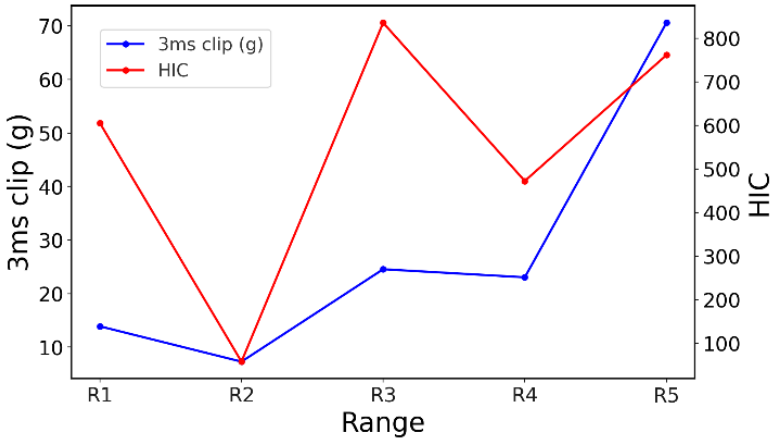

Figure 12. Range results for head injuries

5.3 Verification of Simulation Model Reliability

Since the maximum head injury case is test 9, this paper uses LS-DYNA to simulate the situation (test 9) and verify the accuracy of MADYMO results, as shown in Figure 13. Comparing the head acceleration curves obtained from MADYMO and LS-DYNA during the collision and peak stages, both software show relatively consistent trends in head acceleration. However, in the unloading stage after the collision, MADYMO's results decrease more rapidly, mainly because multibody software lacks structural deformation. As shown in Figure 14, comparing the animation simulation results and the acceleration curves from the two software reveals that, in this case, the results from the finite element software LS-DYNA and the multibody software MADYMO are very close. Therefore, the MADYMO results are reliable and provide a solid foundation for further head injury analysis. More importantly, the computational time in finite element simulation is significantly lengthy. Using LS-DYNA to simulate a full-vehicle collision model containing the THUMS model and a high-version hybrid dummy requires a workstation equipped with a 32-core CPU to run continuously for 30 days, during which time there must be no power interruptions or computational errors. Under current computational resource constraints, this task is almost impossible to complete. In contrast, the MADYMO model requires only 6 hours to complete calculations, is more stable, and has a lower error rate, making it the preferred solution.

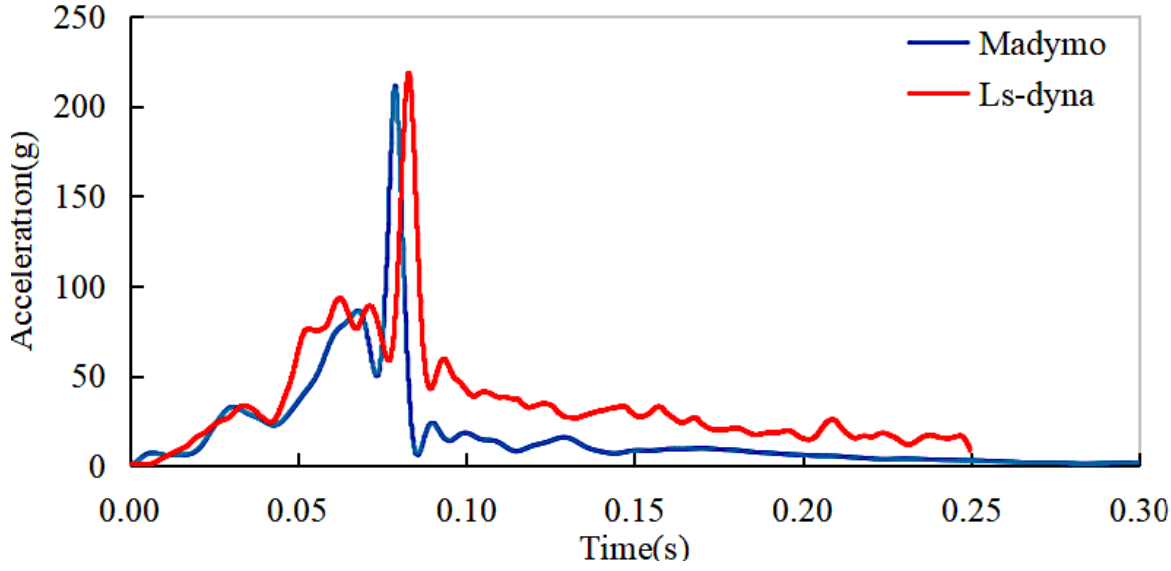

Figure 13. Comparison of orthogonal test 9 Ls-dyna and Madymo simulation results

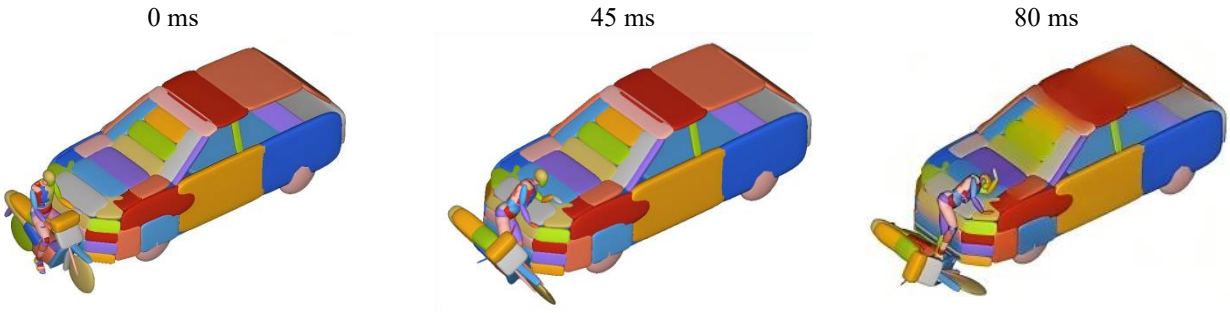

(a) MADYMO

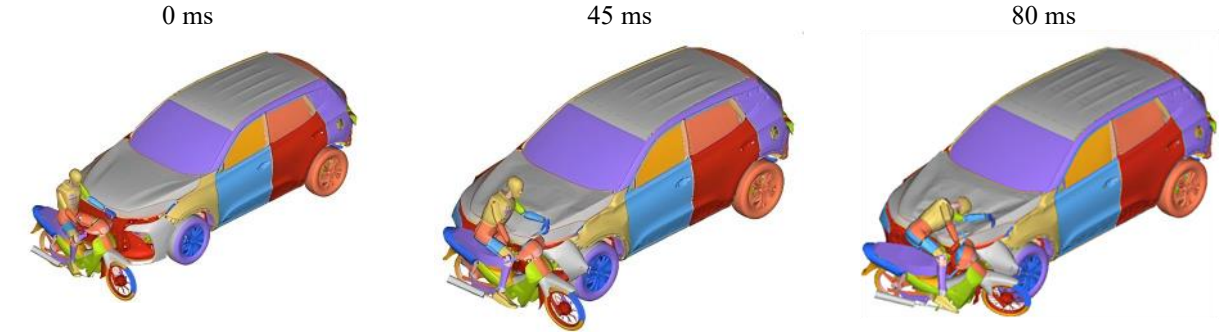

(b) LS-DYNA

Figure 14. Simulation processes for test 9

4. Conclusions

Based on an orthogonal experimental design, this paper systematically studied the influence of multiple factors on rider head injuries in car-PTW frontal collisions, reconstructed typical accident scenarios using multi-rigid-body dynamics models and human dummy models, and analyzed the variation characteristics of HIC15 and the 3 ms Clip. The main conclusions of the study are as follows:

i) By comparing LS-DYNA animations with head acceleration data, the reliability of Madymo in head dynamic response analysis was verified, providing effective support for subsequent research on head injury mechanisms.

ii) Among the PTWs (Powered Two-Wheelers) tested in this study, the impact of PTW type on head injury was relatively minor compared to factors such as vehicle speed and collision angle. Other factors had a far greater influence on injury risk than differences in vehicle type.

iii) Quantitative range analysis confirms that vehicle speed is the dominant factor affecting rider head HIC15, with high vehicle speeds significantly increasing the risk of injury, while collision angle has the most significant impact on 3 ms Clip. In high-speed collisions (80 km/h), rider head injuries reach severe levels (HIC15 increases significantly); in low-speed collisions (10 km/h), the risk of head injury is significantly reduced. Consequently, strictly controlling vehicle speed in mixed-traffic zones is identified as the most effective strategy for reducing rider fatality rates.

Acknowledgements

The authors acknowledge the support provided by the Department of Mechanical and Manufacturing Engineering, Universiti Putra Malaysia, Selangor, Malaysia, and the School of Mechanical and Automotive Engineering, Xiamen University of Technology, Xiamen, China, for research facilities and equipment access for this investigation

Funding

This study was not supported by any grants from funding bodies in the public, private, or not-for-profit sectors.

Declaration of Competing Interest

The author declares no conflicts of interest.

CRediT Authorship Contribution Statement

Yi Pang: (Conceptualization; Writing-original draft; Supervision)
Shaw Voon Wong: (Conceptualization; Validation)
Yong Han: (Conceptualization)
Zulhaidi Jawi: (Investigation)
Yahaya bin Ahmad: (Investigation)
Kean Sheng Tan: (Resources)

Azizan As'arry: (Data curation)
Qiuyun Mo: (Conceptualization; Validation)
Tao Jiang: (Writing – review and editing)

Availability of Data and Materials
The data supporting this study's findings are available on request from the corresponding author.

Ethics Declarations
This study did not involve human participants or animals. Ethical approval was therefore not required.

Generative Artificial Intelligence Declarations
The authors claim that artificially intelligent-assisted technologies, such as generative AI, were not used to generate content, ideas, or theories. We have just utilised AI to enhance readability and refine the language. This was used with extreme human control and oversight. The authors take full responsibility for reviewing and approving the content.

References

[1] V. Haiquan, N. T. Tung, N. A. Ngoc, and D. N. Minh, "Application of Finite Elements to Analysis of Side Collision Problems of Vehicle: A Case Nissan Rogue 2020 SUV Model," *International Journal of Automotive Science and Technology,* vol. 9, no. 1, pp. 81-88, 2025.

[2] K.-H. Song, K. H. Kim, S. Choi, S. Elkosantini, S. M. Lee, and W. Suh, "Comprehensive Safety Index for Road Safety Management System," *Sustainability,* vol. 16, no. 1, p. 450, 2024.

[3] F. Wang, J. Yin, L. Hu, M. Wang, X. Liu, K. Miller, et al. "Should anthropometric differences between the commonly used pedestrian computational biomechanics models and Chinese population be taken into account when predicting pedestrian head kinematics and injury in vehicle collisions in China?," *Accident Analysis & Prevention,* vol. 173, p. 106718, 2022.

[4] Z. Zheng, F. Mo, T. Liu, and X. Li, "A Novel Neuromuscular Head-Neck Model and Its Application on Impact Analysis," *IEEE Transactions on Neural Systems and Rehabilitation Engineering,* vol. 29, pp. 1394-1402, 2021.

[5] S. Yin, J. Li, and J. Xu, "Exploring the mechanisms of vehicle front-end shape on pedestrian head injuries caused by ground impact," *Accident Analysis & Prevention,* vol. 106, pp. 285-296, 2017.

[6] L. F. Gabler, J. R. Crandall, and M. B. Panzer, "Assessment of Kinematic Brain Injury Metrics for Predicting Strain Responses in Diverse Automotive Impact Conditions," *Annals of Biomedical Engineering,* vol. 44, no. 12, pp. 3705-3718, 2016.

[7] G. Crocetta, S. Piantini, M. Pierini, and C. Simms, "The influence of vehicle front-end design on pedestrian ground impact," *Accident Analysis & Prevention,* vol. 79, pp. 56-69, 2015.

[8] J.M. Wang, Z.D. Li, C.S. Cai, Y. Fan, X.B. Liao, F. Zhang, et al., "Parametric analysis of craniocerebral injury mechanism in pedestrian traffic accidents based on finite element methods," *Chinese Journal of Traumatology,* vol. 27, no. 4, pp. 187-199, 2024.

[9] A. Duan, M. Zhou, J. Qiu, C. Feng, Z. Yin, and K. Li, "A 6-year survey of road traffic accidents in Southwest China: Emphasis on traumatic brain injury," *Journal of Safety Research,* vol. 73, pp. 161-169, 2020.

[10] C. E. Baker, X. Yu, S. Patel, and M. Ghajari, "A Review of Cyclist Head Injury, Impact Characteristics and the Implications for Helmet Assessment Methods," *Annals of Biomedical Engineering,* vol. 51, no. 5, pp. 875-904, 2023.

[11] M. Fahlstedt, P. Halldin, and S. Kleiven, "Comparison of multibody and finite element human body models in pedestrian accidents with the focus on head kinematics," *Traffic Injury Prevention,* vol. 17, no. 3, pp. 320-327, 2016.

[12] Q. Wang, B. Yu, Y. Liu, J. Fei, Z. Liu, G. Zhang, et al., "Optimizing vehicle front-end structure for e-bike rider safety: An advanced multi-objective approach using injury prediction models," *Accident Analysis & Prevention,* vol. 207, p. 107754, 2024.

[13] W. Gao, "A study on the cyclist head kinematic responses in electric-bicycle-to-car accidents using decision-tree model," *Accident Analysis & Prevention,* vol. 160, p. 106305, 2021.

[14] Z. Chen, Q. Liu, Z. Zhang, J. Fu, B. Li, and Q. Li, "Effect of riding postures on kinematic responses and head injuries of ETW child passengers," *International Journal of Crashworthiness,* 2024.

[15] C.E. Baker, P. Martin, A. Montemeglio, R. Li, M. Wilson, D.J. Sharp, et al., "Inherent uncertainty in pedestrian collision reconstruction: How evidence variability affects head kinematics and injury prediction," *Accident Analysis & Prevention,* vol. 208, p. 107726, 2024.

[16] K.D. Neumann, V. Seshadri, X.D. Thompson, D.K. Broshek, J. Druzgal, J.C. Massey, et al., "Microglial activation persists beyond clinical recovery following sport concussion in collegiate athletes," *Frontiers in Neurology,* vol. 14, 2023.

[17] Y. Han, Y. He, D. Pan, L. Lin, Y. Chen, and H. Feng, "Effect of different helmets against ground impact based on the in-depth reconstruction of electric two-wheeler accidents," *Computer Methods in Biomechanics and Biomedical Engineering,* vol. 26, no. 4, pp. 460-483, 2023.

[18] T. Brooks, M. Garnich, and M. Jermy, "Sensitivity of material model parameters on finite element models of infant head impacts," *Biomechanics and Modeling in Mechanobiology,* vol. 20, no. 5, pp. 1675-1688, 2021.

[19] Z. B. Zhang, Q. Liu, D. L. Li, Y. Lu, J. Fu, R. Ran, *et al*., "Development of a finite element-multibody coupled model for child brain injury prediction in electric two-wheeler accidents," *Results in Engineering*, p. 109117, 2026.
[20] X. Yang, X. Chen, F. Zhang, T. Yang, J. Kong, X. Liao, *et al*., "Case analysis and finite element analysis of adult head skull fractures in people run over by motor vehicles," *Forensic Sciences Research*, vol. 10, no. 2, p. owaf007, 2025.
[21] L.I. Hai-Yan, L.I.U. Wen-Gang, C.U.I. Shi-Hai, H.E. Guang-Long, X.I.A. Peng, H.E. Li-Juan, et al., "Reconstruction and quantitative evaluation of blunt injury cases by finite element method," *Journal of Forensic Medicine,* vol. 38, no. 4, p. 452, 2022.
[22] L. Shi, Y. Han, H. Huang, J. Davidsson, and R. Thomson, "Evaluation of injury thresholds for predicting severe head injuries in vulnerable road users resulting from ground impact via detailed accident reconstructions," *Biomechanics and Modeling in Mechanobiology,* vol. 19, no. 5, pp. 1845-1863, 2020.
[23] F. Wang, Z. Geng, S. Agrawal, Y. Han, K. Miller, and A. Wittek, "Computation of Brain Deformations Due to Violent Impact: Quantitative Analysis of the Importance of the Choice of Boundary Conditions and Brain Tissue Constitutive Model," Computational Biomechanics for Medicine: From Algorithms to Models and Applications. Cham: Springer International Publishing, pp. 159-173, 2017.
[24] Y. Shim, J. Kim, H. S. Kim, J. Oh, S. Lee, and E. J. Ha, "Intracranial Pressure Monitoring for Acute Brain Injured Patients: When, How, What Should We Monitor," *Korean Journal of Neurotrauma,* vol. 19, no. 2, pp. 149-161, 2023.
[25] E. G. Takhounts, M. J. Craig, K. Moorhouse, J. McFadden, and V. Hasija, "Development of Brain Injury Criteria (BrIC)," *SAE Technical Paper*, 2013.
[26] R. Willinger and D. Baumgartner, "Human head tolerance limits to specific injury mechanisms," *International Journal of Crashworthiness,* vol. 8, no. 6, pp. 605-617, 2003.
[27] E.G. Takhounts, R.H. Eppinger, J.Q. Campbell, R.E. Tannous, E.D. Power, L.S. Shook, "On the development of the SIMon finite element head model," *SAE Technical Paper*, 2003.
[28] B. Yang, X. Zhang, Y. Zheng, P. Zhang, X. Li, J. Wu, *et al*., "Mechanical performance evaluation of negative-poisson's-ratio honeycomb helmets in craniocerebral injury protection," *Materials*, vol. 18, no. 10, p. 2188, 2025.
[29] Y. Zhang, L. Tang, Y. Liu, B. Yang, Z. Jiang, Z. Liu, *et al*., "Consistency assessment of tissue-level brain injury criteria in FEHM," *Computer Methods in Biomechanics and Biomedical Engineering*, pp. 1-15, 2025.
[30] T. Xiong, Q. Luo, Q. Chen, L. Shi, A. Duan, S. Liu, et al., "Development of a repetitive traumatic brain injury risk function based on real-world accident reconstruction and wavelet packet energy analysis," Frontiers in Bioengineering and Biotechnology, vol. 13, p. 1548265, 2025.